Top Catal (2009) 52:1220–1231
DOI 10.1007/s11244-009-9265-6

ORIGINAL PAPER

Modified Lanthanum Catalysts for Oxidative Chlorination of Methane

Elvira Peringer · Michael Salzinger · Markus Hutt · Angeliki A. Lemonidou · Johannes A. Lercher

Published online: 28 April 2009

Abstract Mixtures of LaOCl and $LaCl_3$ are promising catalysts for oxidative chlorination of methane to methyl chloride. The influence of metal dopants such as Co, Ni and Ce, which form stable chlorides under anticipated reaction conditions, on physicochemical and catalytic properties was explored. The presence of markedly redox-active dopants such as cobalt and cerium lead to a higher rate of methane conversion. However, the formed methyl chloride is strongly adsorbed and directly oxidized to CO leading to low methyl chloride selectivity. Doping with nickel weakens, in contrast, the interaction with methyl chloride leading to high methyl chloride selectivity.

Keywords Methane oxidative chlorination · $LaCl_3$ · LaOCl · Methyl chloride · Methane

1 Introduction

The direct functionalization of methane is very challenging due to its tetrahedral geometry and the strong C–H bonds (439 kJ mol^{-1}) [1, 2]. In consequence, thermodynamic boundaries dictate that substituting hydrogen in methane for another element requires coupling to a strong exothermic (oxidative) reaction. As the resulting products are chemically more reactive than methane, over-oxidation, and over-functionalization of methane are frequent problems encountered.

A promising approach is the selective catalytic methane conversion to methyl chloride via oxidative chlorination (Eq. 1). Methyl chloride is an important reactant in a number of chemical processes, such as in the production of silicon [3] or methanol [4]. Potentially, methyl chloride could also be used as the basis of the synthesis of higher hydrocarbons, whereby the HCl set free in the process can be reused for the oxidative chlorination [4–6].

$$CH_4 + HCl + 0.5O_2 \rightarrow CH_3Cl + H_2O \quad (1)$$

Recent reports [7, 8] showed that $LaCl_3$ is a promising stable catalyst for the conversion of methane to methyl chloride by oxidative chlorination using oxygen and HCl. It is superior to the well-established copper based catalysts [9–12], which are unstable and volatile under reaction conditions. The latter also catalyze the formation of chlorine via the Deacon reaction, initiating radical gas phase chlorination with low selectivity towards methyl chloride.

$LaCl_3$ catalyzes the reaction without a change in the oxidation state of lanthanum through a surface catalyzed reaction with a transient hypochlorite species as active site [7]. The hypochlorite species is formed on the chloride surface by reaction with oxygen from the gas phase. Methane exchanges hydrogen for positively charged chlorine atom of the transiently formed hypochlorite carbonium ion like transition state. This leads to a chlorine atom vacancy. Hydrogen chloride is then regenerating the surface via substituting the OH-group formed in the exchange with Cl^- generating water. Selectivities for methyl chloride above 90% can be obtained between 300 and 360 °C at low

Angeliki A. Lemonidou is on leave from the Department of Chemical Engineering, Aristotle University Thessaloniki.

E. Peringer · M. Salzinger · M. Hutt · A. A. Lemonidou · J. A. Lercher (✉)
Department of Chemistry, Technische Universität München, Lichtenbergstr. 4, 85747 Garching, Germany
e-mail: johannes.lercher@ch.tum.de

A. A. Lemonidou
Department of Chemical Engineering, Aristotle University Thessaloniki, POB 1517, 54006 Thessaloniki, Greece

conversions. As the conversion increases, the selectivity to CH_2Cl_2 increases, with $CHCl_3$ and CCl_4 being notably absent in the product mix.

It should be noted that the active catalyst $LaCl_3$ is in equilibrium with LaOCl (Eq. 2). Under reaction conditions, the surface is partially de-chlorinated.

$$LaCl_3 + H_2O \rightleftharpoons LaOCl + 2HCl \quad (2)$$

Especially above 500 °C, $LaCl_3$ releases HCl in the presence of water and is partially transformed to LaOCl. Oxidative chlorination can also be understood as a dynamic transformation between $LaCl_3$ and LaOCl. Chlorine is provided to the reaction in a Mars van Krevelen type mechanism [8]. Without HCl present in the gas phase, $LaCl_3$ transforms gradually into LaOCl.

Previously, the rate of methane conversion has been positively correlated to the specific surface area [13]. This indicates that the same acid site density exists on the active materials studied. The question arises now, if the reactivity of the active sites (involving La^{3+}) can be modified by other metal cations. To probe this, LaOCl catalysts were modified with metal chloride salts such as $CoCl_2$, $NiCl_2$, and $CeCl_3$, which show a melting point higher than 550 °C. The impact of $CeCl_3$ is particularly interesting; it is a lanthanide metal, but contrary to La it can change its formal oxidation state. The so prepared catalysts are characterized and tested for the synthesis of chloromethane from methane, HCl and oxygen.

2 Experimental

2.1 Catalyst Preparation

The $LaCl_3$ catalysts were prepared in situ in an HCl flow from LaOCl precursors. The LaOCl precursor was prepared by precipitation at room temperature using ammonium hydroxide (20% NH_4OH, Merck) and a solution of lanthanum(III)chloride heptahydrate (99%, Merck) in ethanol. After drop-wise addition of the base to the solution, the suspension was stirred for 1 h to facilitate complete precipitation. The precipitate obtained by centrifugation was washed twice with an excess of ethanol to remove the residual base. Finally, the gel was freeze dried and calcined for 8 h at 550 °C in synthetic air, using an increment of 5 °C min^{-1} and a flow of 200 mL min^{-1}.

LaOCl was impregnated by incipient wetness impregnation with an aqueous solution of cobalt dichloride hexahydrate (Riedel de Haën, 99%), nickel dichloride hexahydrate (Merck, 98%), or cerium trichloride heptahydrate (Sigma-Aldrich, 99.9%), respectively. In each case, LaOCl was loaded with 5 mol% of the metal chloride. Due to the low solubility of cerium chloride the impregnation had to be repeated three times until the desired cerium content was reached. The materials were freeze dried after impregnation.

LaOCl was initially activated in He flow (40 mL min^{-1}) at 550 °C for 1 h using an increment of 10 °C min^{-1}. Subsequently, the material was converted to $LaCl_3$ in situ by reacting with HCl (20 vol.% HCl in He, total flow 50 mL min^{-1}) at 400 °C for 14 h. The samples are named Me/LaOCl independent of their state of chlorination indicating the precursor material.

2.2 Physicochemical Characterization

The crystallographic structure of the LaOCl precursors and resulting $LaCl_3$ catalysts was determined by XRD with a Philips X'Pert Pro System ($CuK_{\alpha 1}$-radiation) at 45 kV/40 mA. The measurements were performed with a step scan of 0.017° min^{-1} from 10° to 70° 2θ. The morphology and particle size of the LaOCl precursor was examined by scanning electron microscopy using a JEOL 500 SEM-microscope (accelerating voltage 25 kV). Before recording the SEM images, the sample was outgassed for two days at room temperature and sputtered with gold.

BET surface area and pore volume were determined by nitrogen adsorption at 77.4 K using a PMI automated BET Sorptometer. The mesopore size distribution was obtained from the desorption branch of the isotherm using the Barret–Joyner–Halenda (BJH) method, the micropore volume was obtained from the desorption branch of the isotherm using the Horvath–Kawazoe (HK) method [14]. Prior to measurement, the LaOCl samples were outgassed in vacuum (10^{-3} Pa) at 250 °C for 2 h.

2.3 Thermogravimetry

The thermal stability of the materials was investigated by thermogravimetric methods in a modified Setaram TG-DSC 111 system. The samples were pressed into thin wafers and subsequently broken into small platelets. Approximately 17 mg of these platelets were charged into the quartz sample holder of the balance. The samples were heated in vacuum (1×10^{-6} bar) with a temperature increment of 5 °C min^{-1} to 750 °C. Changes in weight were observed and the gases evolved were analyzed with a Balzers quadrupole mass spectrometer.

In order to understand the correlation between the product distribution and the catalytic activity of the prepared catalysts, the oxygen uptake was investigated by using TG/DSC. Approximately 50 mg of each catalyst, pressed and sieved, were filled in the quartz sample holder and activated for 1 h at 550 °C in vacuum. After activation, the sample was cooled down to 100 °C and oxygen (500 mbar) was introduced in the system and kept at

100 °C for 0.5 h. Then, the temperature was increased up to 350 °C with a temperature increment of 5 °C min^{-1} and hold at 350 °C for 0.5 h for oxygen adsorption. After the absorption period, the system is again cooled down to 100 °C with a rate of 5 °C min^{-1} and hold at 100 °C for 1 h in O_2 atmosphere. The oxygen uptake was determined by the weight increase of the sample.

2.4 Catalytic Tests

The in situ prepared $LaCl_3$ sample was tested in methane oxidative chlorination using a fixed-bed quartz tubular reactor filled initially with 500 mg of LaOCl precursor (0.3–0.6 mm size fraction). The temperature of the reactor oven was controlled by a thermocouple placed above the catalyst bed. The gas flows (CH_4, O_2, HCl, N_2, He) were adjusted using mass flow controllers. Helium was used as a diluent, and nitrogen as an internal standard. The reactor outlet was analyzed online by a Siemens Maxum Edition II gas chromatograph. After analysis, the gases were passed through a NaOH scrubber to remove unreacted HCl. The lines of the setup were coated with glass lining and heated to 150 °C to prevent water condensation and corrosion. CH_4 (purity 4.5) and O_2 (4.5) were provided from Messer Griesheim and HCl (2.8), N_2 (5.0) and He (4.6) by Air Liquide. All gases were used without further purification.

The dependence of the product distribution on methane conversion was evaluated by varying the space velocity, changing the total flow from 5 to 25 mL min^{-1} using a stoichiometric ratio of reactants (CH_4:HCl:O_2:He:N_2 = 2:2:1:4:1) at 475 °C. Before starting the analysis of the reaction products, the catalyst was stabilized for 8 h at 475 °C. Each space velocity was maintained for 1.5 h to ensure stable operating conditions.

The overall dependence of the product distribution on temperature was probed by a temperature programmed reaction (TPR) varying the reacting temperature from 200 to 650 °C with an increment of 1 °C min^{-1} and feeding reactants at a stoichiometric ratio (CH_4:HCl:O_2:He:N_2 = 2:2:1:4:1) with a total flow of 10 mL min^{-1}.

The ability of the catalyst to accept chlorine was studied with temperature programmed chlorination experiments. A mixture of He:HCl (4:1; 50 mL min^{-1}) was passed over the sample while increasing the temperature from room temperature to 650 °C with 3 °C min^{-1}. The HCl uptake was monitored by GC analysis.

2.5 In Situ Raman Measurements

In situ Raman measurements were performed with an industrial LaOCl catalyst provided by The Dow Chemical Company in a tubular fix-bed quartz reactor system. The conditions for activation, chlorination and reactions were similar to those of the catalytic tests. In situ Raman spectra were collected at ambient conditions through a hole in the oven with a Holoprobe Kaiser Optical spectrometer equipped with a holographic notch filter, CCD camera and 532 nm laser. The Raman spectra were collected at different reaction temperatures with an exposure time of 1 s and 50 accumulations.

3 Results

3.1 Chemical Composition, Morphology and Structural Aspects

The results of the N_2 physisorption and concentration of the dopant metal in the fresh and used catalysts are summarized in Table 1. After catalytic tests at 475 °C for 15 h, the concentration of dopant metals decreased in all cases. The most significant loss of dopant was observed for Ni/LaOCl. Loss of dopants was also visually observed via the coloration of the inert reactor packing downstream of the catalyst bed, i.e., the yellow color in the case of nickel and the blue color in the case of cobalt. The loss in metal is attributed to the significant vapor pressures of the metal chloride salts [15] and the facilitation of the surface migration of the chlorides by the abundance of HCl in the gas phase.

The parent LaOCl had the highest BET surface area of 17 m^2 g^{-1}. The surface areas and the pore volumes were lower after impregnation with metal salts (9–13 m^2 g^{-1}). The N_2 physisorption for the samples after 14 h chlorination at 400 °C showed that the BET surface area was further decreased, e.g., to 8 m^2/g for Ce/LaOCl. The decrease in specific surface area is attributed to the always observed restructuring of the materials during the chlorination of LaOCl to $LaCl_3$.

The samples as prepared had a wide distribution of particles with irregular shape and diameters between 2.5 and 20 μm. The particles were characterized by a fragmented surface and were composed of agglomerated nanoparticles (see Fig. 1a). The morphology of the impregnated samples was hardly changed and showed the same agglomerated nano-particles like the parent LaOCl, as shown in Fig. 1b for Ce/LaOCl. The similar shape also indicates that the added salts are deposited in the pore structure as expected from incipient wetness impregnation and the modification procedure does not lead to pronounced particle agglomeration.

3.2 Thermogravimetry

The thermal stability of the synthesized catalysts was investigated by thermogravimetry. For the parent LaOCl the main desorbing compounds were water (m/z = 18) and

Table 1 N_2 physisorption and AAS results of the fresh catalysts and dopant loss after reaction at 475 °C

Sample	BET s. area (m^2/g)	Pore volume (cm^3/g)	Dopant content (Me mol%)	Dopant content (Me wt%)]	Dopant loss (%)
LaOCl	17	0.060	–	–	–
Co/LaOCl	13	0.056	4.7	1.45	8
Ni/LaOCl	9	0.045	5.0	1.53	24
Ce/LaOCl	9	0.030	5.1	3.72	14

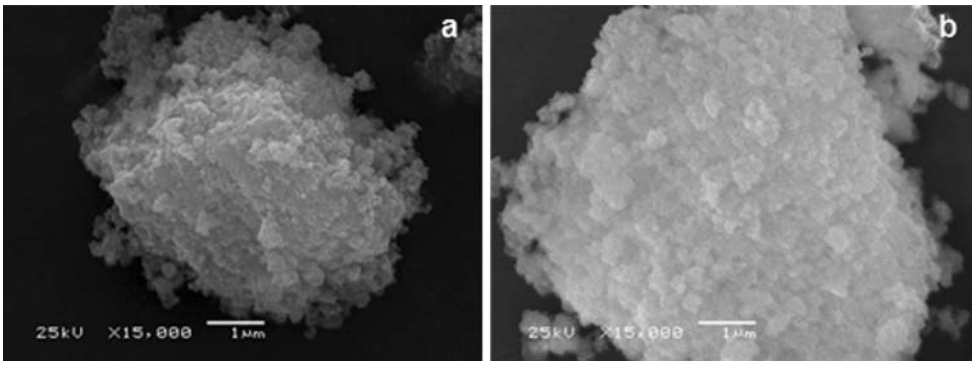

Fig. 1 SEM photographs (15,000 fold enlargement) of **a** parent LaOCl and **b** Ce/LaOCl

HCl ($m/z = 36$). Desorption of water was observed in the temperature range 60–425 °C (see Fig. 2). A maximum was found at 275 °C and a smaller peak at 125 °C. At 285 °C HCl ($m/z = 36$) began to evolve. It showed a maximum at 360 °C and decayed in a long tail until the end of the measurement. The HCl evolution is attributed to the partial hydrolysis of LaOCl to La_2O_3. Besides HCl also Cl_2 release ($m/z = 70$) and CO_2 ($m/z = 44$) were observed. The formation of carbon dioxide is attributed to the decomposition of residual lanthanum carbonate on the surface. However, the weight loss due to Cl_2 and CO_2 liberation was negligible compared to the weight loss by water and HCl. The total weight loss of the parent LaOCl in the whole temperature range was 3.6 wt.%. The thermogravimetric results of all samples are summarized in Table 2. The release of water and hydrogen chloride of Ni/LaOCl was only slightly higher compared to the parent LaOCl. The other impregnated samples released approximately twice the amount of water and HCl compared to the parent LaOCl. Co/LaOCl desorbed even the triple amount of water. For all catalysts, around 75% of the total HCl evolution occurred below the generally applied activation temperature of 550 °C.

During activation in vacuum at 10^{-7} mbar, evolution of the metal salts was also observed by mass spectrometry between 300 and 450 °C. This is attributed to the significant vapor pressure of some metal chloride salts, e.g., at 350 °C nickel chloride has a vapor pressure of 2.3×10^{-6} mbar [15]. This explains also the remarkably higher total weight loss of the metal impregnated catalyst compared to the parent LaOCl. The difference between the total weight loss and the loss due to water and hydrogen chloride release showed the same trend as the dopant loss after reaction (see Table 1).

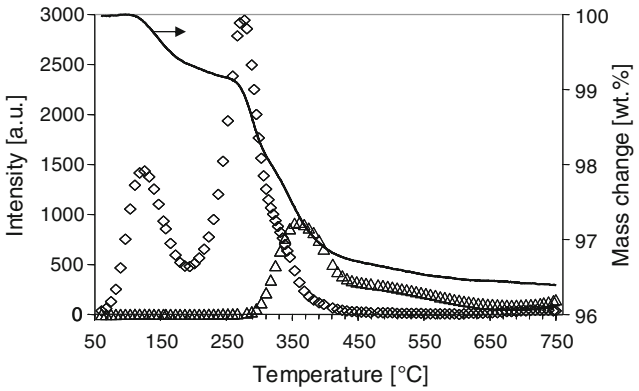

Fig. 2 TGA profile of LaOCl in the temperature range of 50–750 °C (*diamond*: $H_2O = m/z$ 18; *triangle*: HCl = m/z 36)

The ability of the catalysts to bind and activate oxygen on the surface was investigated by thermogravimetry. Depending on the type of the metal dopant, the concentration of oxygen uptake varied (Table 3). While the parent LaOCl adsorbed 1.49×10^{-3} mmol O_2 g_{cat}^{-1}. Co/LaOCl had a significantly higher uptake compared to the oxygen uptake of the parent LaOCl.

3.3 Catalytic Conversion of Methane

3.3.1 Activity and Selectivity

The catalytic performance in oxidative chlorination of methane was tested at 475 °C varying the weight hourly

Table 2 Weight loss between 50 and 750 °C during heating in a dynamic vacuum of 10^{-7} mbar

Sample	H_2O release (wt%)	HCl release (wt%)	Total weight loss[a] (wt%)
LaOCl	1.7	1.2	3.6
Co/LaOCl	5.1	2.6	8.7
Ni/LaOCl	1.9	1.4	5.6
Ce/LaOCl	3.3	2.6	7.3

[a] Besides H_2O and HCl, the total weight loss also includes the release of Cl_2, CO_2 and metal compounds

Table 3 Oxygen uptake per catalyst weight

Sample	O_2 uptake (mmol g_{cat}^{-1})	Relative to LaOCl
LaOCl	1.49×10^{-3}	1.00
Co/LaOCl	2.45×10^{-3}	1.65
Ni/LaOCl	1.45×10^{-3}	0.98
Ce/LaOCl	1.79×10^{-3}	1.20

space velocity (WHSV), after chlorination of the catalysts at 400 °C. At a WHSV of 1.45 h^{-1} the rate of methane conversion is 0.58 mmol h^{-1} g_{kat}^{-1} over the parent LaOCl sample. Doping with Co and Ce enhances the catalytic activity and rates of 4.27 and 2.74 mmol h^{-1} g_{kat}^{-1}, respectively, are observed. Doping with Ni reduces the catalytic activity and a rate of methane conversion of 0.16 mmol h^{-1} g_{kat}^{-1} is found.

The dependence of the product yields on methane conversion over the parent LaOCl is shown in Fig. 3. Methyl chloride was always the main product and was formed with the highest selectivity. The dotted line illustrates the yield for 100% selectivity. Already at low methane conversion the initial yield of methyl chloride (dashed line) was lower than 100%.

The main by-product formed was carbon monoxide. It is important to note that the selectivity to methyl chloride is lower and the initial oxidation of methane to CO is higher than in the material reported in [7, 8] We speculate at present that the materials prepared here, retain a part of the formed methyl chloride species on their surface. This leads to a catalytic pathway that favors the reaction of the (partially chlorinated) methyl species with the hydroxy groups formed during the initial steps or with oxygen present in the sample. Thus, the deviation of the initial methyl chloride yield from 100% selectivity is attributed to the direct oxidation of adsorbed methyl chloride to carbon monoxide. It is important to note that in addition to this pathway the readsorption of methyl chloride, additional chlorination, and oxidation of the readsorbed species may take place, which causes a further decrease of the methyl chloride selectivity and increase of the CO and methylene chloride selectivity at higher methane conversion, respectively. The deviation of the methyl chloride yield to the

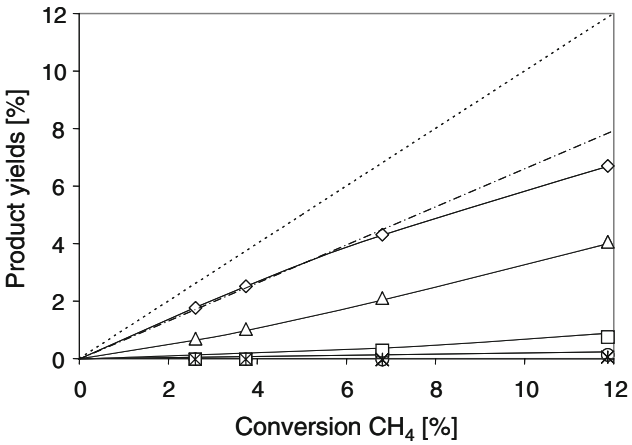

Fig. 3 Product yields as a function of methane conversion over LaOCl at 475 °C with stoichiometric flow CH_4:HCl:O_2:He:N_2 = 2:2:1:4:1 (*diamond*: CH_3Cl; *square*: CH_2Cl_2; *circle*: $CHCl_3$; *triangle*: CO, *six-spoked asterisk*: CO_2; *dotted-broken line*: initial CH_3Cl yield; *dotted line*: 100% selectivity line)

initial yield became stronger at higher methane conversion due to the increasing methylene chloride yield. This indicates that the (undesired) formation of CH_2Cl_2 proceeded via a consecutive reaction by the further chlorination of methyl chloride. Higher chloromethanes, as $CHCl_3$ (maximum yield 0.2%) and CCl_4, were only detected in trace amounts. The deep oxidation product CO_2 was hardly detected even at higher conversions.

Cerium modification led to a marked increase in activity. However, the selectivity and, thus, the yield to methyl chloride over Ce/LaOCl was relatively low (Fig. 4). In the observed conversion range (up to 31%), carbon monoxide was the main product (CO yield up to 19%) followed by methyl chloride, methylene chloride and carbon dioxide. Chloroform was formed in very low concentration with a maximum yield of 2%. However, the yield was significantly higher compared to the parent LaOCl catalyst. Tetrachloromethane was formed only in negligible amounts. The formation of CO by the preferred reaction of strongly bound (partly chlorinated) surface species with hydroxy groups and oxygen is more pronounced over Ce/LaOCl compared to LaOCl. The positive deviation of the CO yield to the initial yield is attributed to the

formation of higher chlorinated methane which is more reactive towards further oxidation to carbon monoxide and HCl.

Co/LaOCl exhibited also a high methane conversion ranging up to 31% with even higher yield up to 24% towards CO (results not shown). Over this catalyst the methyl chloride yield reached a maximum of 4.3% at 27.5% methane conversion. The Co/LaOCl catalysts showed the highest yield towards $CHCl_3$ and CCl_4 of all catalysts with a maximum of 3% for chloroform and 0.4% for tetrachloromethane.

Ni/LaOCl was less reactive than the parent LaOCl. This catalyst reached a maximum methane conversion of around 5% under the present reaction conditions. Over Ni/LaOCl, methyl chloride was the main product and was very selectively formed and approached a methyl chloride yield of 4% (Fig. 5). The yield towards methylene chloride was relatively low, while the CO yield reached 0.6%. Carbon dioxide, chloroform and tetrachloromethane were not observed. In contrast to the other studied catalysts, the initial methyl chloride selectivity is close to 100%.

The correlation of methane conversion and CH_3Cl selectivity at 475 °C for all catalysts is depicted in Fig. 6. The comparison of the methyl chloride selectivity at around 5% methane conversion showed that Ni/LaOCl was the most selective catalyst. The Ni/LaOCl catalyst reached 86% selectivity towards methyl chloride whereas the parent LaOCl reached only 70% methyl chloride selectivity. In contrast, Ce/LaOCl and Co/LaOCl exhibited at 5% methane conversion only a methyl chloride selectivity of 53 and 43%, respectively.

In order to increase the reactivity of Ni/LaOCl the reaction temperature was increased to 580 °C and runs were conducted at WHSV ranging from 0.48 to 2.91 h^{-1}

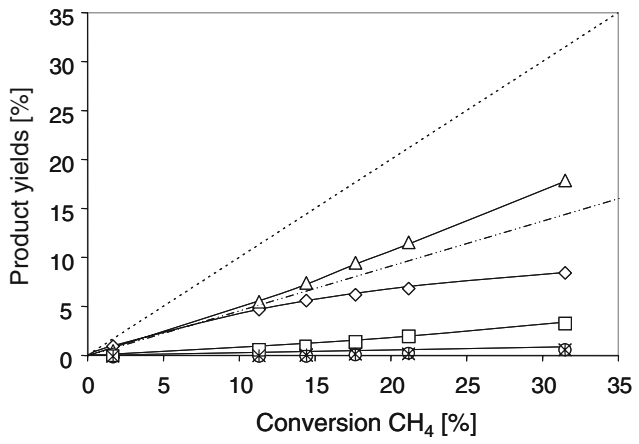

Fig. 4 Product yields as a function of methane conversion over Ce/LaOCl at 475 °C with stoichiometric flow CH_4:HCl:O_2:He:N_2 = 2:2:1:4:1 (*diamond*: CH_3Cl; *square*: CH_2Cl_2; *circle*: $CHCl_3$; *triangle*: CO; *six-spoked asterisk*: CO_2; *dotted-broken line*: initial CO yield; *dotted line*: 100% selectivity line)

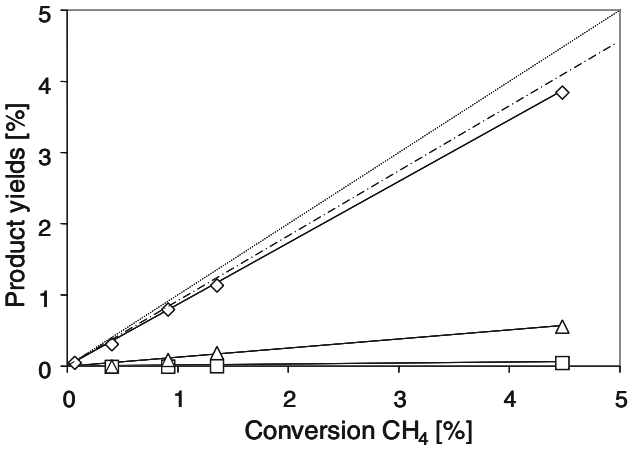

Fig. 5 Product yields as a function of methane conversion over Ni/LaOCl at 475 °C with stoichiometric flow CH_4:HCl:O_2:He:N_2 = 2:2:1:4:1 (*diamond*: CH_3Cl; *square*: CH_2Cl_2; *triangle*: CO; *dotted-broken line*: initial CH_3Cl yield; *dotted line*: 100% selectivity line)

(filled squares in Fig. 6). In fact, at this temperature methane conversions between 6.6 and 23.6% were obtained, which are close to the conversions obtained with Ce/LaOCl. In contrast to Ce/LaOCl methyl chloride was the main product for Ni/LaOCl at these conversions. The selectivity towards methyl chloride was in the range between 79 and 62%. Carbon monoxide was formed with low selectivity, not surpassing 20%. Chloroform and carbon dioxide were formed in only negligible amounts.

3.3.2 Temperature Programmed Reaction

In order to explore the reactivity of the catalysts as a function of temperature, TPR was performed with the chlorinated catalysts. While such an experiment cannot account for deactivation or transient modifications of the

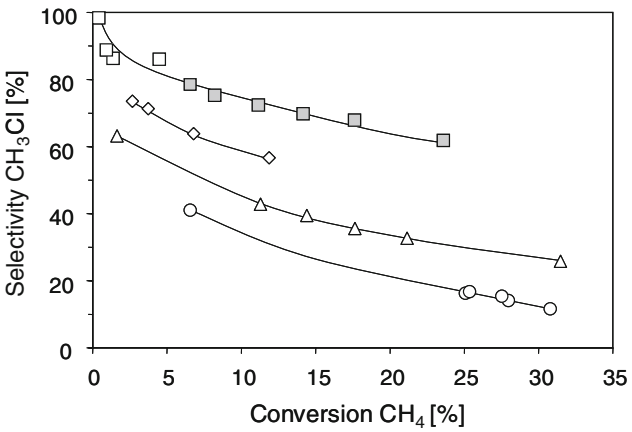

Fig. 6 CH_3Cl selectivity vs. CH_4 conversion at 475 °C with stoichiometric flow CH_4:HCl:O_2:He:N_2 = 2:2:1:4:1 (*diamond*: LaOCl; *circle*: Co/LaOCl; *triangle*: Ce/LaOCl; *white square*: Ni/LaOCl; *filled square*: Ni/LaOCl at 580 °C)

catalyst, it probes the general reaction sequence and, thus, is used to explore the trends in reactivity including the onset of the reaction and the thermal stability with respect to the dechlorination of the catalyst. The temperature dependence of the reactant conversions and the product yields over the parent LaOCl are provided in Fig. 7a and b, respectively.

The temperature dependence of the reactant conversion and product yields can be divided into three areas. At low temperatures (370–425 °C), methane conversion was low and methyl chloride was formed as a primary product with high selectivity. With the increase of methane conversion, also the oxygen conversion started to increase. However, the hydrogen chloride conversion was still zero and started to increase at higher temperatures. At higher methane conversion (425–550 °C), the hydrogen chloride conversion was almost equal to the methane conversion implying that the catalyst surface was regenerated with hydrogen chloride. At temperatures between 425 and 550 °C, carbon monoxide is formed and increased in parallel to methyl chloride. This indicates that methyl chloride did not totally desorb from the surface, but was directly further oxidized to carbon monoxide. In addition, methylene chloride was formed and the increase of the methyl chloride yield with temperature was reduced accordingly. The oxygen conversion in this temperature range was much higher than the methane conversion, which is attributed to the oxygen consumption for oxidation of the chlorinated products to carbon monoxide. From 525 °C on, the catalyst surface started to dechlorinate to LaOCl according to the equilibrium between $LaCl_3$ and LaOCl (Eq. 2). The restructuring of the catalyst surface was accompanied with the abrupt increase in carbon monoxide yield and also a slight increase of the yield of higher chlorinated products. At temperatures above 545 °C, also the bulk of the catalyst started to dechlorinate to LaOCl, which was characterized first by the decrease of the HCl consumption during the TPR, which eventually turns into an HCl outlet concentration that is higher than the inlet concentration. Using the chlorine mass balance, we exclude that this HCl evolution was the result of HCl excess initially adsorbed on the sample.

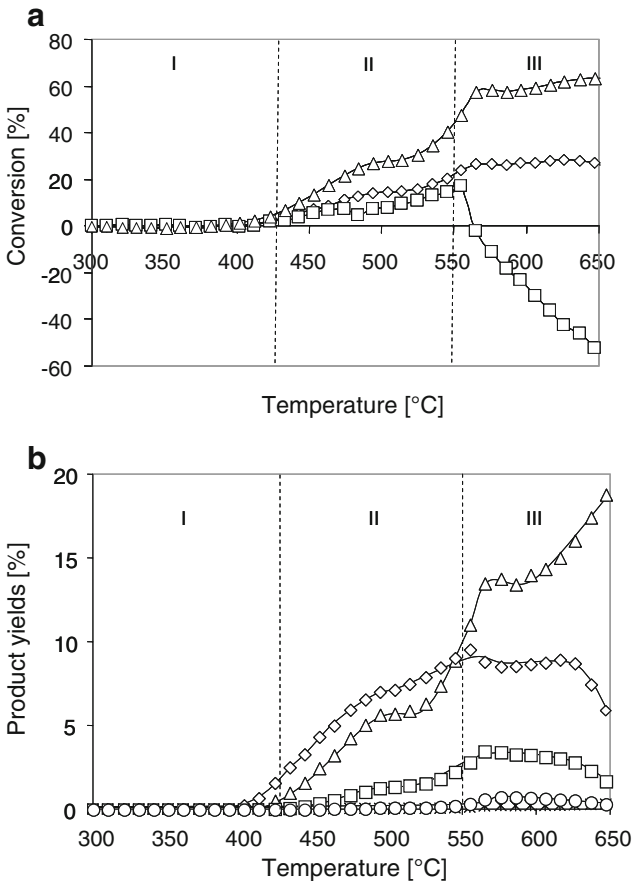

Fig. 7 **a** Profile of the reactant conversion during TPR (1 °C min^{-1}) over the parent LaOCl with stoichiometric flow CH_4:HCl:O_2:He:N_2 = 2:2:1:4:1 (*diamond*: CH_4; *square*: HCl; *triangle*: O_2). **b** Profile of the product yields during TPR (1 °C min^{-1}) over the parent LaOCl with stoichiometric flow CH_4:HCl:O_2:He:N_2 = 2:2:1:4:1 (*diamond*: CH_3Cl; *square*: CH_2Cl_2; *circle*: $CHCl_3$; *triangle*: CO; *six-spoked asterisk*: CO_2)

The methane conversion remained constant from the start of dechlorination, whereas the oxygen conversion increased slightly. When chlorine has been almost depleted from the surface ($T > 615$ °C), the CO yield increased due to further oxidation of chlorinated products on a surface leaner in chlorine. As a result, the rate of formation of methyl chloride and methylene chloride decreased. The TPR profiles of Ce/LaOCl are shown in Fig. 8a and b, respectively. Methyl chloride was detected from 370 °C on in parallel with increasing methane and oxygen conversion. With a short delay also the HCl conversion started to increase. Methyl chloride was the only product formed until 390 °C, at which temperature also carbon monoxide appeared. Higher chlorinated products such as methylene chloride and chloroform were formed from 450 °C on. Above 450 °C, the readsorption of methyl chloride appears to be favored, which was concluded from the constant formation of methyl chloride and the parallel increase of the CH_2Cl_2 and CO formation rate. The oxygen conversion increased in a more pronounced way than methane conversion, which is related to the high formation of carbon monoxide. The dechlorination of the catalyst started at 540 °C. Above that threshold, the methane and oxygen consumption remain almost constant indicating that the increasing reaction rate must be compensated by decreasing concentration of active sites. At 620 °C the HCl release stopped and the HCl conversion showed a reversion to positive values. The yield of carbon monoxide showed a

steep increase until 650 °C at the expense of the chlorinated products especially of CH_2Cl_2 and $CHCl_3$.

The TPR profiles of Co/LaOCl (not shown here) showed the same trends as Ce/LaOCl. However, over Co/LaOCl a higher yield of carbon monoxide was observed, which showed a very steep increase with temperature. The methyl chloride yield is lower compared to Ce/LaOCl. The start of dechlorination of Co/LaOCl was observed at 530 °C.

The TPR profiles of Ni/LaOCl are shown in Fig. 9a and b. The start of methane and oxygen conversion over Ni/LaOCl was 25 °C higher compared to the parent LaOCl. However, methyl chloride is the only formed product until 500 °C and the CH_3Cl yield was steadily increasing till 650 °C (Fig. 9b). Above 500 °C CH_2Cl_2, $CHCl_3$, and CO were formed. In contrast to the other modified catalysts, methyl chloride was always the main product and the CO yield was much lower than the CH_2Cl_2 yield even at higher temperatures. The dechlorination of Ni/LaOCl started at 585 °C. In contrast to the parent LaOCl and Ce/LaOCl, the methane conversion continued to increase further even after the start of dechlorination until 640 °C. Also the product yields seemed unaffected from the dechlorination.

The consumption and evolution of HCl during the TPR for the parent LaOCl and the doped catalysts are shown in Fig. 10. The start of dechlorination and the total amount of released HCl is summarized in Table 4. It should be kept in mind that $LaCl_3$ is in equilibrium with LaOCl. The equilibrium is shifted towards LaOCl in the presence of water (produced during reaction) with HCl being released (Eq. 2). Fully chlorinated $LaCl_3$ heated in a He flow with 3 °C min^{-1} to 650 °C did not release HCl. Thus, we conclude that dechlorination requires the presence of water. The parent LaOCl catalyst started to dechlorinate at 545 °C, Co/LaOCl and Ce/LaOCl already at 530 and 540 °C, respectively. In contrast, Ni/LaOCl started to dechlorinate at 585 °C.

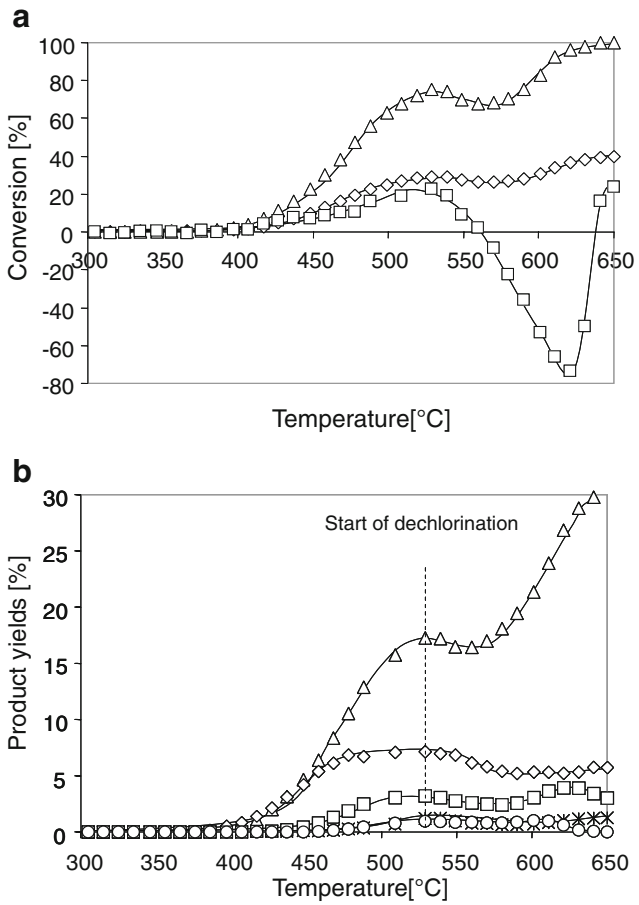

Fig. 8 **a** Profile of the reactant conversion during TPR (1 °C min^{-1}) over Ce/LaOCl with stoichiometric flow CH_4:HCl:O_2:He:N_2 = 2:2:1:4:1 (*diamond*: CH_4; *square*: HCl; *triangle*: O_2). **b** Profile of the product yields during TPR (1 °C min^{-1}) over Ce/LaOCl with stoichiometric flow CH_4:HCl:O_2:He:N_2 = 2:2:1:4:1 (*diamond*: CH_3Cl; *square*: CH_2Cl_2; *circle*: $CHCl_3$; *triangle*: CO; *six-poked triangle*: CO_2)

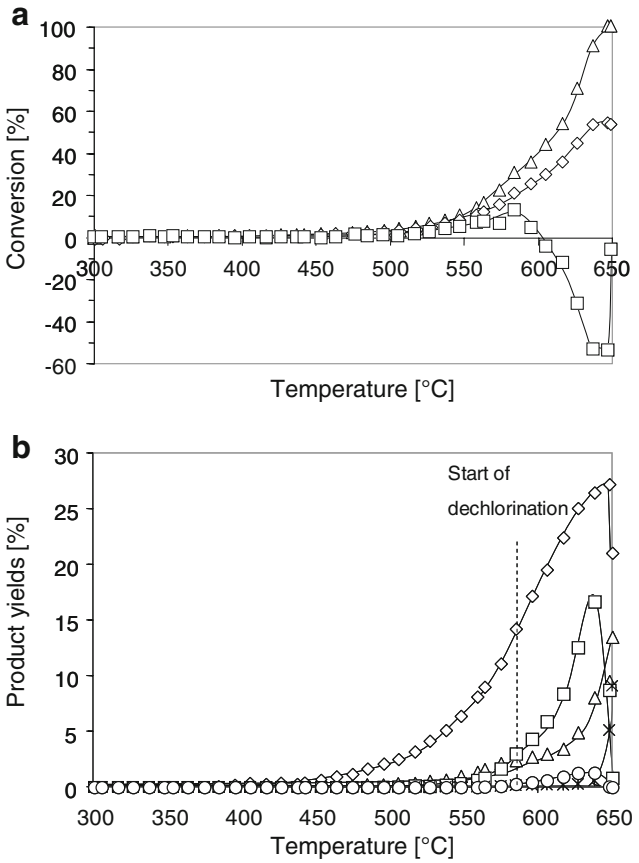

Fig. 9 **a** Profile of the reactant conversion during TPR (1 °C min^{-1}) over Ni/LaOCl with stoichiometric flow CH_4:HCl:O_2:He:N_2 = 2:2:1:4:1 (*diamond*: CH_4; *square*: HCl; *triangle*: O_2). **b** Profile of the product yields during TPR (1 °C min^{-1}) over Ni/LaOCl with stoichiometric flow CH_4:HCl:O_2:He:N_2 = 2:2:1:4:1 (*diamond*: CH_3Cl; *square*: CH_2Cl_2; *circle*: $CHCl_3$; *triangle*: CO; *six-spoked asterisk*: CO_2)

Table 4 Start of dechlorination and HCl release during TPR (1 °C min^{-1})

Sample	Start of dechlorination (°C)	HCl release (mmol g^{-1})	Relative to LaOCl
LaOCl	545	0.15	1.0
Co/LaOCl	530	0.25	1.6
Ni/LaOCl	585	0.13	0.9
Ce/LaOCl	540	0.24	1.6

The parent LaOCl showed an HCl release of 7.6×10^{-5} mol. This amount does not correspond to a fully transformation of lanthanum chloride to lanthanum oxychloride indicating that the bulk of the catalyst remains unchanged. The highest HCl release was detected for Co/LaOCl, followed by Ce/LaOCl, whereas Ni/LaOCl showed the least release of HCl. It should be noted, that the HCl release of the metal chloride doped samples cannot only originate from the metal chloride used for impregnation, as the detected amount was much higher. Note that the observed trend in the onset of HCl release corresponds to the trend in the activity for oxidative chlorination.

Over all catalysts the yield of the desired CH_3Cl reached a certain level and was then almost constant over the whole temperature range (Fig. 11). Whereas the Ni/LaOCl showed a lower yield of methyl chloride up to 500 °C, beyond this temperature a dramatic increase of the methyl chloride yield with a maximum at 650 °C was observed, even though the catalyst has already started to dechlorinate.

3.4 XRD Analysis

The crystal structures of the samples were investigated by X-ray diffraction. The X-ray diffractograms showed that the impregnation method did not influence the LaOCl crystal structure (Fig. 12). The diffraction pattern for tetragonal LaOCl was present in all samples with same intensity ratios and width as the parent LaOCl catalyst [16].

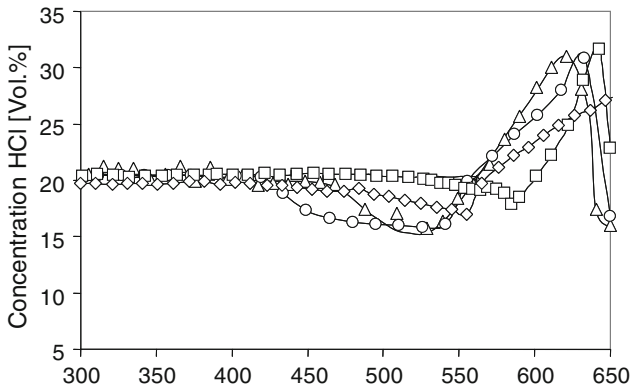

Fig. 10 Profile of HCl consumption/evolution during TPR (1 °C min^{-1}) with 20 vol.% HCl in the feed (*diamond*: LaOCl; *circle*: Co/LaOCl; *square*: Ni/LaOCl; *triangle*: Ce/LaOCl)

After chlorination at 400 °C for 14 h, the parent LaOCl sample was fully transformed into $LaCl_3$, while for Ni/LaOCl the transformation was not complete (see Fig. 13), i.e., $LaCl_3$ and LaOCl were present approximately in a ratio of 3:1. This indicates that the bulk of the particles was not fully chlorinated in line with the results of the temperature programmed chlorination. As expected, the equilibrium shifted under reaction conditions towards LaOCl during the TPR and, thus, only the LaOCl phase was observed with the used catalyst (see Fig. 13c).

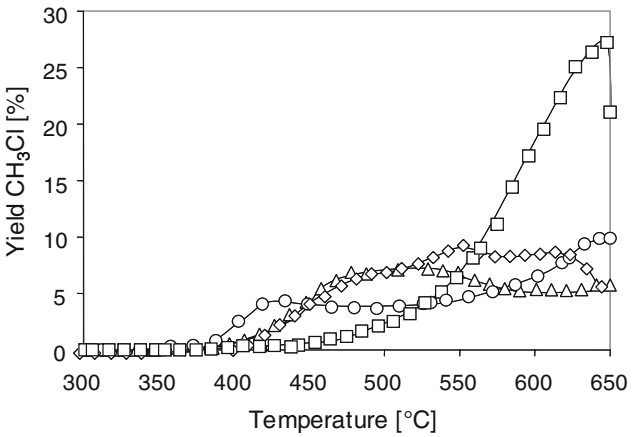

Fig. 11 Methyl chloride yield during TPR (1 °C min^{-1}) with stoichiometric flow CH_4:HCl:O_2:He:N_2 = 2:2:1:4:1 (*diamond*: LaOCl; *circle*: Co/LaOCl; *square*: Ni/LaOCl; *triangle*: Ce/LaOCl)

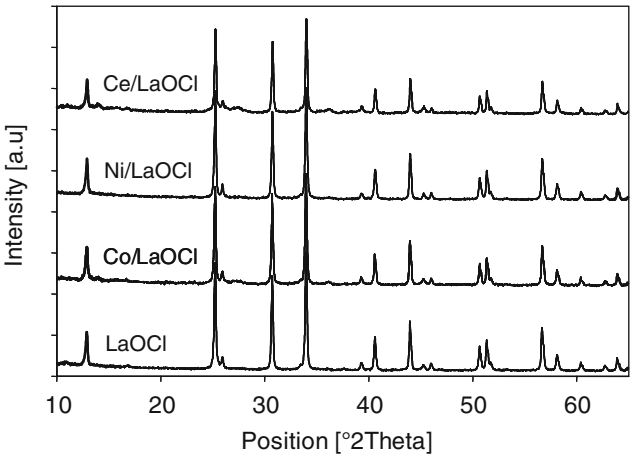

Fig. 12 XRD diffractograms of the parent LaOCl precursor and the metal modified catalysts

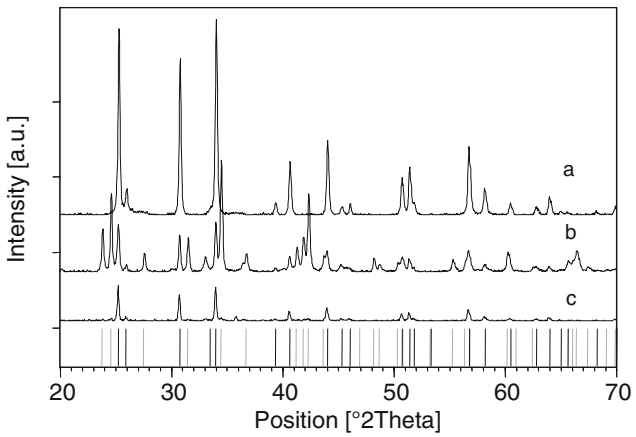

Fig. 13 XRD analysis of Ni/LaOCl (a) after calcination, (b) after chlorination for 14 h at 400 °C, (c) after TPR (*thick vertical line*: calculated pattern for LaOCl JCPDS-file 73-2063; *thin vertical line*: calculated pattern for $LaCl_3$ JCPDS-file 73-0479)

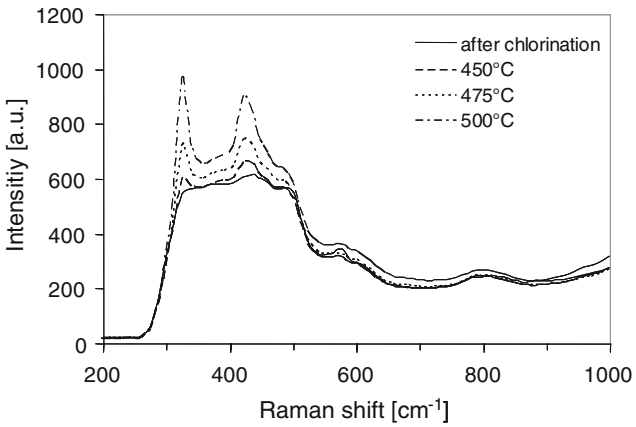

Fig. 14 In situ Raman spectra of pure LaOCl (industrial sample) after chlorination and during reaction and at different temperatures with stoichiometric flow CH_4:HCl:O_2:He = 2:2:1:5 (532 nm laser)

3.5 In Situ Raman Spectroscopic Measurements

The transformation of $LaCl_3$ to LaOCl on the surface under reaction conditions using stoichiometric flow of CH_4:HCl:O_2 = 2:2:1 at different temperatures were also investigated by in situ Raman spectroscopy (Fig. 14). At the start of the measurements, bands of LaOCl were present. Due to the cut off at 280 cm^{-1} only the bands at 330 and 430 cm^{-1} associated with the motion of the oxygen atoms were observed [8]. After chlorination at 400 °C, the LaOCl bands disappeared indicating the chlorination of the catalyst to $LaCl_3$. The Raman bands of $LaCl_3$ are all below 219 cm^{-1} and were thus not visible [17].

Under oxidative chlorination conditions at 450 °C weak bands of LaOCl were observed indicating partial dechlorination of the surface under reaction conditions. The LaOCl bands gained in intensity with increasing the reaction temperature to 500 °C suggesting that the equilibrium between $LaCl_3$ and LaOCl is shifted towards LaOCl.

4 Discussion

The impregnation of LaOCl with metal chloride salts influences the physicochemical properties and the catalytic performance of the catalytic materials for the oxidative chlorination of methane. The thermostability of the chloride is reduced by impregnation, as indicated by the more pronounced HCl release of Co/LaOCl and Ce/LaOCl during activation in vacuum. The pronounced release of HCl from these samples parallels with their higher water content compared to the parent LaOCl. Around 75% of HCl liberation is below the applied activation temperature of 550 °C. Thus, during thermal activation, part of LaOCl is hydrolyzed and chlorine defect sites or even minor amounts of La_2O_3 are generated. It is speculated that these defects are the initial sites of chlorine uptake during chlorination of the thermally activated LaOCl.

The modification of LaOCl with cobalt and cerium has a marked influence on the activity in oxidative chlorination of methane. The activity towards methane conversion varies with the redox activities of the chloride used, i.e., it is higher for Co/LaOCl and Ce/LaOCl and lower for Ni/LaOCl than the parent LaOCl. Interestingly, it is not influenced by the specific surface area of the catalyst precursor or of the chlorinated catalyst (see Table 1). This is in contrast with the finding that the rate of methane conversion correlates linearly with the specific surface area of $LaCl_3$ [13]. The absence of such a relation in the present case indicates that the chemical effects dominate by far over the specific surface area.

Chemisorption of molecular oxygen on the activated and chlorinated materials is critical for the formation of the transient active species on LaOCl or $LaCl_3$, i.e., $Cl^{\delta+}$ in an OCl^- anion as shown by DFT calculations [7]. Under steady state conditions, the adsorption of oxygen can, therefore, not cause the formation of stable OCl^-, but transient species could cause a synproportionation of Cl^- and Cl^+ to Cl_2. This could desorb or remain at the catalyst surface. Thus, oxygen adsorption capacity is conceptually a descriptor of catalytic activity. Indeed, the ability to adsorb oxygen decreases in the sequence Co/LaOCl > Ce/LaOCl > LaOCl ~ Ni/LaOCl, identical with the ranking of activities of the materials. However, the higher concentration of the surface hypochlorite species also leads to a more extensive chlorination as evidenced by the marked level of chloroform production with Co/LaOCl and Ce/LaOCl.

Methyl chloride is the primary product over all catalyst, followed by carbon monoxide. It should be emphasized that the CH_3Cl and the CO yields are correlated for the different catalysts. Especially, the Ni containing sample has a relatively low activity for activating methane, but is highly selective towards methyl chloride compared to the other catalysts. The low rate of activation and the low degree of multiple chlorinations and total oxidation implies a low concentration of the active sites over these catalysts and the near absence of oxygen on the surface. In line with this, for the highly active catalysts Co/LaOCl and Ce/LaOCl CO is the main product. As CO is formed also as primary product, we infer that methyl and methyl chloride species are retained strongly on the surface and react with hydroxyl groups on these materials. In addition, the facile formation of CO indicates that the concentration of oxygen on the surface of these catalysts must be substantial.

Methyl chloride (formed as primary product) may also be readsorbed undergoing further chlorination as wells as oxidation to CO. This is indicated by the simultaneous decrease of the methyl chloride selectivity and the increase of CO and methylene chloride selectivity with increasing methane conversion. It should be noted that the tendency for oxidation increases with the chlorine content of the adsorbed species [18]. Thus, materials having higher activity will also show a higher tendency for multiple chlorination and oxidation.

The TPR and especially the evolution of HCl allows insight into the relative mechanistic steps at various temperatures. When the methyl chloride formation starts, HCl conversion is still negligible indicating that the surface chlorine atoms are used as a chlorine source. Thus we conclude that the role of HCl is limited to regenerate the surface via addition of Cl^- and the formation of water [8]. However, as shown with in situ Raman measurements, the catalyst surface is not fully regenerated and LaOCl bands with low intensity are already visible at 450 °C. Therefore, a partially dechlorinated, LaOCl like, surface is concluded to be characteristic of the state of the catalyst under reaction conditions. At a certain temperature, the HCl profile shows a reverse to negative HCl conversions. At this point, the rate for methane chlorination (Eq. 1) is equal to the rate of dechlorination of the catalyst surface (Eq. 2). At higher temperatures the rate of dechlorination is higher than the rate for chlorination of the catalyst and the catalyst surface dechlorinates to LaOCl state. In consequence, methane conversion remains constant even though the temperature is steadily increasing due to the decreasing amount of active sites. The impact of the reaction temperature on the reaction rate is, thus, compensated by the lower concentration of active sites due to dechlorination of the surface. Once conversion to LaOCl is completed HCl is used again as chlorination agent.

The start temperature of dechlorination is affected by doping with different metal salts and directly correlates with the activity at 475 °C. The most active catalysts, Co/LaOCl and Ce/LaOCl, start to dechlorinate at much lower temperatures than the parent LaOCl. This effect can be explained by the amount of water produced, which is necessary to shift the equilibrium towards LaOCl. The more active catalysts Co/LaOCl and Ce/LaOCl are able to supply the required amount of water in order to shift the equilibrium towards LaOCl at a lower reaction temperature than Ni/LaOCl. When the transformation of $LaCl_3$ to LaOCl is complete, the selectivity towards CO increases, whereas the selectivity towards chlorinated products decreases. This is attributed to the increased activity of LaOCl in catalytic destruction of higher chlorinated products as previously shown [18–21]. Therefore, the selectivity to methylene chloride decreases more drastically than the selectivity of methyl chloride.

Ni/LaOCl shows a totally different HCl–TPR profile. The maximum HCl conversion reaches only 12% and the start of dechlorination is at higher temperatures due to the low activity. Even though the start temperature of HCl release is higher and the overall release is lower compared to the parent LaOCl, the dechlorination seems to be complete at 640 °C. From these results we conclude that Ni/LaOCl is in a less chlorinated state, which results in a lower concentration of active sites and thus a lower activity. The low chlorination degree of Ni/LaOCl is confirmed by the XRD analysis after chlorination (see Fig. 13). The fact that the rates of methane conversion and methyl chloride formation increase further, even after the start of dechlorination suggest that the low concentrations of active sites and the weak interaction of the formed methyl chloride with the surface prevent the formation of higher chlorinated products and the further oxidation to CO.

5 Conclusions

$LaCl_3$ is a unique catalyst for the oxidative functionalization of methane with HCl to methyl chloride. The addition of metal dopants to $LaCl_3$ has different effects on the activity in oxidative chlorination. The modification with strongly redox active cobalt and cerium chloride causes a remarkable increase of catalytic activity, which is related to the enhanced oxygen adsorption capacity, i.e., to a higher concentration of the active site OCl^-. The formed (partially chlorinated) methyl species are strongly adsorbed on the surface of these catalysts and further oxidized to CO leading to a low selectivity to methyl chloride. Doping with a less redox-active compound, such as nickel chloride, leads to a reduced activity compared to the parent LaOCl material, due to the lower degree of chlorination of the

surface. Due to this lower concentration of chlorine on the surface, it appears that both the degree of chlorination and the retention on the surface is lowered via this strategy. Thus, future selective catalysts targeting low degree of chlorination of methane and low loss through total oxidation will be based on dopants that stabilize a lower chlorine concentration on the surface of the chloride materials.

Acknowledgments A. Van der Heijden of NRSC-Utrecht is gratefully acknowledged for performing the in situ Raman measurements and the fruitful discussions. The authors are grateful to X. Hecht for BET measurements and M. Neukamm for SEM and AAS measurements. This work was partially financed by The Dow Chemical Company. Partial financial support and fruitful discussion in the framework of the network of excellence IDECAT-WP5 (NMP3-CT-2005-011730) is also gratefully acknowledged.

References

1. Golden DM, Benson SW (1969) Chem Rev 69(1):125
2. Crabtree RH (1995) Chem Rev 95(7):2599
3. Bablin JM, Lewis LN, Bui P, Gardner M (2003) Ind Eng Chem Res 42(15):3532
4. Periana RA, Mironov O, Taube D, Bhalla G, Jones CJ (2003) Science 301(5634):814
5. Noronha LA, Souza-Aguiar EF, Mota CJA (2005) Catal Today 101(1):9
6. Sun Y, Campbell SM, Lunsford JH, Lewis GE, Palke D, Tau LM (1993) J Catal 143(1):32
7. Peringer E, Podkolzin SG, Jones ME, Olindo R, Lercher JA (2006) Top Catal 38(1–3):211
8. Podkolzin SG, Stangland EE, Jones ME, Peringer E, Lercher JA (2007) J Am Chem Soc 129:2569
9. Garcia CL, Resasco DE (1989) Appl Catal 46(2):251
10. Kenney CN (1975) Catal Rev Sci Eng 11(2):197
11. Rouco AJ (1995) J Catal 157(2):380
12. Wattimena F, Sachtler WMH (1982) Stud Surf Sci Catal 7:816
13. Peringer E, Tejuja C, Salzinger M, Lemonidou AA, Lercher JA (2008) Appl Catal A 350(2):178
14. Horvath G, Kawazoe K (1983) J Chem Eng Jpn 16(6):470
15. Weast RC (ed.) (1975–1976) Handbook of chemistry and physics, 56th edn. CRC Press Inc, Cleveland, p D-183
16. Hölsä J, Lastusaari M, Valkonen J (1997) J Alloys Compd 262:299
17. Weckhuysen BM, Rosynek MP, Lunsford JH (1999) Phys Chem Chem Phys 1(13):3157
18. Van der Avert P, Weckhuysen BM (2004) Phys Chem Chem Phys 6(22):5256
19. Van der Heijden AWAM, Garcia Ramos M, Weckhuysen BM (2007) Chem Eur J 109(1–2):97
20. Van der Heijden AWAM, Bellière V, Alonso LE, Daturi M, Manoilova OV, Weckhuysen BM (2005) J Phys Chem B 109:23993
21. Van der Avert P, Weckhuysen BM (2002) Angew Chem Int Ed 41(24):4730